Jestr

Journal of Engineering Science and Technology Review 16 (6) (2023) 27 - 35

Research Article

JOURNAL OF
Engineering Science and Technology Review

www.jestr.org

Multivariate Optimization of Machining Forces Generated by End Milling of Hardox® 450 Steel Under Different Lubricooling Conditions

Émerson dos Santos Passari* and André João de Souza

Engenharia Mecânica - Processos de Fabricação, Laboratório de Automação em Usinagem (LAUS) – UFRGS

Received 15 May 2023; Accepted 20 October 2023

Abstract

Hardox® is a martensitic steel characterized by high hardness and resistance to abrasive wear, increasingly used in the agricultural, mining, and transport industries. In some specific contexts, its application requires the fabrication of components through the machining processes. In addition, optimizing cutting parameters and correctly applying lubricooling techniques are essential to enhancing productivity while always seeking to reduce environmental damage. Thus, this work investigates the cutting parameters' effects on the active and passive forces and the static and dynamic portions of the machining force in the end milling of Hardox® 450 with PVD-TiAlN coated carbide inserts under different lubricooling conditions (dry, flood, and nanofluid-based reduced quantity lubrication "NF-RQL"), aiming to perform its multivariate optimization. As expected, the results showed that the depth of cut (a_p) is the most significant parameter, followed by feed per tooth (f_z) and the interaction between them. Although the force values obtained by lubricooling conditions were similar, NF-RQL can provide a higher material removal rate (1456 cm^3/min) than dry (1116 cm^3/min) and flood (1019 cm^3/min) conditions.

Keywords: Hardox® 450 end milling, Nanofluid-based reduced quantity lubrication, Machining forces, Multivariate optimization.

1. Introduction

The foundations of industrial production are based on reducing costs, increasing productivity, and seeking to guarantee the quality of the process through the dimensional and geometric accuracy of products. Furthermore, the constant search for technologies used in new materials aims to develop components with high mechanical resistance, low cost, excellent durability, etc. Thus, it is essential to evaluate the economic value of the material and its machinability. In this context, the SSAB-Oxelösund developed in the 1970s the Hardox® steel which has high hardness and resistance to abrasive wear [1]. Since this material also has toughness similar to several alloys applied in the industry, these properties allow its application in replacing conventional alloys as it promotes an increase in the component life-cycle or even the reduction of their specific weight. This replacement has been used mainly in the mining, agricultural and transport industries, resulting in savings related to durability (high resistance to mechanical abrasion) or fuel-consumption reduction when Hardox® intends to decrease the vehicle's mass [2][3]. These steels are produced by hot rolling, followed by quenching and tempering heat treatment. This treatment results in a tempered-martensitic microstructure that, when combined with added alloy elements, generates high hardness, toughness, ductility, and wear resistance [3]. Classified according to its mechanical properties (especially hardness, which is commonly indicated in the material's nomenclature), Hardox® 450 has a nominal hardness of 450 HBW and a yield strength of 1250 MPa [2][4]. Therefore, Hardox® 450 presents difficulties in machining without an adequate cutting tool [5], cutting parameters [6], and lubricooling method [7].

Milling is one of the machining processes used to manufacture Hardox® steel components [8], characterized by interrupted cutting. The machining force (F_U) results from the cutting action and is intrinsically related to the workpiece material, tool material, tool geometry, and the presence or absence of a lubricoolant. The variation in chip thickness modifies the forces generated during tool action, which may increase when machining hardened materials due to higher shear resistance [9]. The shear zones and material strength are the main factors influencing F_U [10]. In general, all factors that contribute to facilitating chip sliding over the tool rake face act to decrease F_U. Chip formation usually occurs three-dimensionally, and therefore, the F_U has three orthogonal components (F_x, F_y, F_z) that act directly on the cutting edge and, consequently, on the structure of the machine tool [9]. The measurement and analysis of the machining force (F_U) during the process are relevant factors for evaluating tool wear, vibrations, energy consumption, etc. High force values commonly derive from the wrong choice of machining parameters, which may result in vibrations that compromise the machined surface [6, 11] or cause premature failures in the cutting tool [5, 12, 13]. Different works about milling Hardox® do not agree with the recommended cutting tool material due to the material properties, such as high hardness and high manganese content, which increases the work-hardening tendency. Although these material properties can be classified into four grades (steel, stainless steel, cast iron, and hardened steel) [8], the use of ISO-S grade (superalloys) for finishing end milling of Hardox® is also found in the literature [6].

The cutting fluid in machining reduces the friction between the tool-chip and tool-workpiece interfaces,

*E-mail address: emerson.passari@gmail.com
ISSN: 1791-2377
doi:10.25103/jestr.166.04

decreases the temperature in the cutting zone, and increases the tool life [14]. The traditional application of cutting fluid in abundance (flow rates above 300 L/h) is the most common technique employed in end milling [15]. However, this flood condition represents a high environmental impact, risk to operators' health and increased machining costs. These costs denote up to 16% of the total machining cost, and the charge of treating and disposing of non-biodegradable fluids can be two to four times higher than the purchase price [16]. Furthermore, the flood application is not an effective method to form a lubricating film, especially at higher cutting speeds, because it can sometimes not reach the cutting zone efficiently [17]. Thus, the growing concern about the environmental impact caused by the machining process encouraged the research of alternative methods less aggressive to nature without prejudicing the previously established productivity requirements [18].

Regarding clean machining, dry cutting is the first choice for milling, mainly because it avoids the thermal fatigue in the tool. Then, strategies based on the reduced or minimum quantity lubrication (RQL or MQL) applied directly to the cutting zone are presented as less aggressive and economical solutions than the flood condition [17, 19, 20]. According to Chinchanikar et al. [21], MQL generally produced the best results in the end milling of hardened steels, reducing machining force, tool wear rate, and surface roughness compared to dry and flood conditions. Recent advances in nanotechnology have allowed new possibilities in machining processes. Nanoparticles of different materials (e.g., molybdenum disulfide, manganese sulfide, graphene) constitute a nanofluid (NF) when mixed with cutting fluid through a specific homogenization process [22]. With this approach, adding multilayer graphene nanoplatelets (MLG) to cutting fluid may improve the effect of MQL/RQL since MLG has excellent thermal dissipation and lubrication characteristics and high resistance to oxidation and corrosion [14]. Finally, SSAB [4, 8] recommends flood condition for turning and drilling Hardox® 450, but there is no indication for milling, generating uncertainty about the best technique for this machining process.

Due to the diverse factors that influence the end milling of Hardox® 450, it is necessary to have a suitable design and analysis of the experiment aiming to define the controllable input variables and the response output variables. As mentioned above, high forces are usually the result of improper choice of cutting parameters, which can generate vibrations that compromise the machined surface finish or cutting tool state. Thus, the parameters' optimization can collaborate to reduce the machining force and increase the stability of the milling process under different lubricooling techniques. Therefore, the Box-Behnken Design (BBD) is recommended to be a statistical optimization method that works simultaneously on a set of independent input factors to obtain the best levels that exert influence on the response of a given process [5][23][24][25].

In this context, the present work seeks to optimize the cutting parameters to reduce machining forces and evaluate the application of a multilayer graphene-based nanofluid in the end milling of Hardox® 450, comparing its performance with dry and flood conditions. The innovation brought by this study lies in applying multivariate analysis and optimization techniques to improve the machinability of Hardox steel and in the evaluation of lubrication techniques seeking to reduce environmental impact, including the use of nanofluids in decreasing quantities. This information can help develop better machining practices for similar materials with high hardness and resistance to abrasive wear for different industrial sectors.

2. Materials and Methods

Table 1 shows the chemical composition of the Hardox® 450 steel used according to the SSAB manufacturer's inspection certificate number 850210068 (May 2019), compared to the values acquired by the SPECTROMAXx™ LMX06 arc/spark optical emission spectrometry analyzer equipment. This comparison shows that the measured values are similar to certificated values, evidencing the chemical control in its manufacture [3]. Furthermore, the hardness value, measured by the Pantec hardness tester, was (443 ± 22) HBW.

Table 1. Chemical composition of Hardox® 450 steel (%wt.)

Element	C	Si	Mn	P	S	Cr	Ni	Mo	B
Certificated	0.163	0.207	1.083	0.011	0.001	0.093	0.096	0.020	0.016
Measured	0.166	0.240	1.193	0.005	<0.001	0.045	0.072	0.018	0.029

End milling was performed in the CNC ROMI Discovery 308 machining center with a maximum power of 5.5 kW and a maximum spindle of 4000 rpm. A Walter Tools end-milling cutter with a 20 mm nominal diameter and two positive rhombic TiAlN + Al2O3 PVD-coated carbide inserts with a 0.8 mm tool-tip radius were used. Rectangular sheet (100 x 90 x 6.35 mm) workpieces were defined for fixing on the Kistler piezoelectric dynamometer. Six runs (samples) with 34 mm length were machined in each workpiece using different combinations of the controllable factors for each lubricooling condition. **Fig. 1** shows the experimental setup.

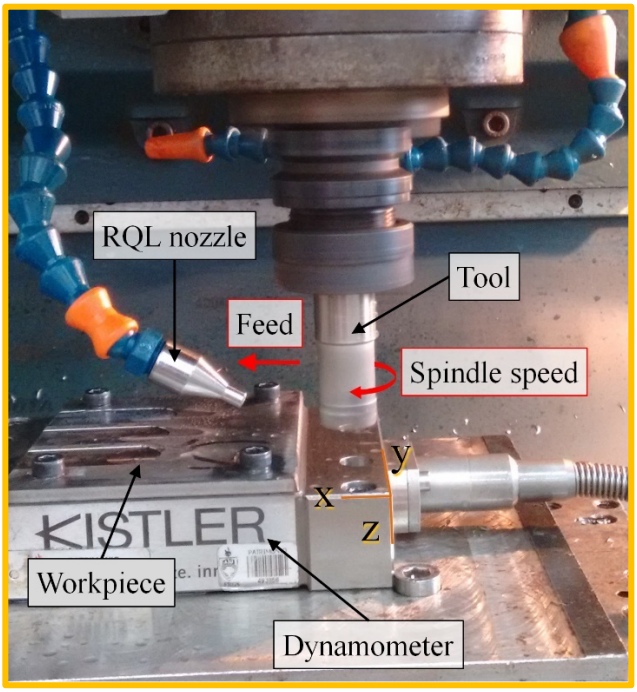

Fig. 1. Experimental setup

Three lubricooling conditions were evaluated: flood, NF-RQL and dry. The flood condition used the oil-free bio-lubricant Bondmann® BD-Fluid B90 with a 1:20 dilution at a flow rate of 540 l/h. The nanofluid (NF) used in the experiment is a Quimatic® Jet integral water-based synthetic

fluid, with the addition of multilayer graphene nanoplatelets (MLG), dispersed at a concentration of 0.05% wt by an ultrasonic homogenizer. The MLG nanoplatelets, with an area of 1 to 10 μm² and thickness of 1 to 20 nm, were obtained by exfoliation of thermally expanded natural graphite with acids at high temperature, preceded by an ultrasonic process for mechanical exfoliation [26]. After homogenization of the NF, just simple stirring is sufficient. The NF-MLG was applied in reduced quantity lubrication (RQL) via the Tapmatic® Nebulizer IV at a 2.0 l/h flow rate and 300 kPa pressure in the compressed air line. The dry condition did not employ any lubrication-cooling process.

The force signals in the three orthogonal directions (F_x, F_y, F_z) were acquired by a KISTLER 9129AA piezoelectric dynamometer and conditioned using a KISTLER 5070A10100 charge amplifier. The Measurement Computing® PCIM-DAS 1602/16 board performed the analogic data acquisition at a rate of 5 kS/s. Finally, the digital signals of F_x, F_y, and F_z were processed by LabVIEW® 9.0 software. After that, the machining force (F_U) was determined using Eq. 1. Similarly, the active and passive forces (F_a and F_p) were calculated by Eq. 2 and Eq. 3, respectively. The static portion of the machining force (μF_U) was obtained from the arithmetic mean of the calculated values (Eq. 4), and the dynamic portion (ΔF_U) was generated based on a normal statistical distribution for a 95% confidence interval (Eq. 5). The data samples of N = 20,000 points, collected in the stable machining region (disregarding the cutter entry and exit regions), were used to calculate the response variables (Eq. 2 to Eq. 5).

$$F_U\,(\mathrm{N}) = \sqrt{F_x{}^2 + F_y{}^2 + F_z{}^2} = \sqrt{F_a{}^2 + F_p{}^2} \tag{1}$$

$$F_a\,(\mathrm{N}) = \sqrt{F_x{}^2 + F_y{}^2} \tag{2}$$

$$F_p\,(\mathrm{N}) = F_z \tag{3}$$

$$\mu F_U\,(\mathrm{N}) = \frac{\sum_{i=1}^{N} F_{Ui}}{N} \tag{4}$$

$$\Delta F_U\,(\mathrm{N}) = \pm 1{,}96 \cdot \sqrt{\frac{\sum_{i=1}^{N} (F_{Ui} - \mu F_U)^2}{N}} \tag{5}$$

Response surface methodology (RSM) is a collection of statistical techniques useful for modeling and analyzing problems in which several variables influence the response of interest. This methodology also quantifies the relationship between the controllable factors (input parameters) and the obtained response surfaces. Box-Behnken Design (BBD) is a statistical optimization method that consists of a factorial analysis with incomplete block designs based on the RSM [27]. The chosen input controllable factors were cutting speed v_c (m/min), feed per tooth f_z (mm/tooth), and axial depth of cut a_p (mm). The cutting parameters (v_c, f_z, a_p) were established as continuous variables and evaluated at three levels, selected within the range of values recommended by SSAB Oxelösund [4, 8]. The experiment was combined and randomized using BBD via statistical software Minitab® 18, with one run for each combination and three runs for the central point (3#, 8#, 13#), totaling 15 runs for each lubricooling condition [23], as presented in **Tab. 2**. Moreover, one cutting-edge pair was used for each lubricooling condition (or 15 runs) to reduce the effect of tool wear on the response variables.

Table 2. Sequence run order

Run	1	2	3#	4	5	6	7	8#	9	10	11	12	13#	14	15
v_c	120	80	100	100	100	100	80	100	80	120	120	80	100	100	120
a_p	1.2	0.4	0.8	1.2	0.4	0.4	0.8	0.8	1.2	0.4	0.8	0.8	0.8	1.2	0.8
f_z	0.10	0.10	0.10	0.05	0.15	0.05	0.05	0.10	0.10	0.10	0.15	0.15	0.10	0.15	0.05

It should be noted that uncontrollable factors (e.g., tool wear) can affect the system performance and slightly change the measurement results. This noise is the random error associated with the experiment. According to Black [28], machining involves high strains combined with high strain rates, and the variety of options for controllable factors results in infinite combinations. However, Cica et al. [29] mentioned that through optimization, the ideal cutting conditions could meet a specific machining criterion, be it higher productivity, better finishing, or cost reduction.

3. Results and Discussions

Fig. 2 shows the plots of the static (μF_U) and dynamic (ΔF_U) portions of the machining force. The lowest force value ($\mu F_U \pm \Delta F_U$) is evidenced for the three lubricooling conditions in run 6 (middle v_c, low a_p, and low f_z) and the highest in run 14 (middle v_c, high a_p, and high f_z). Thus, as expected, increasing a_p and/or f_z results in an almost linear increase of μF_U and ΔF_U values due to the growth of the cross-sectional area. [9][19][30]. There was no significant variation between the measured force values when comparing the influence of each lubricooling condition. However, considering the average of the mean values, the flood condition generated slightly higher force values (238.9 ± 158.4 N) compared to NF-RQL (230.0 ± 147.4 N) and dry cutting (231.1 ± 146.4 N) probably due to the increase of work hardening with the rise of the flood cooling capacity [1]. The growth of force in flood compared to the dry machining was about 3.5% for μF_U and 8.0% for ΔF_U.

Fig. 3 shows the plots of the active (F_a) and passive (F_p) components of the machining force. The effect of the cross-sectional area on F_a is also noted; however, the highest F_p value was measured in run 11 (high v_c, middle a_p, and high f_z) and the lowest in run 2 (low v_c, low a_p, and middle f_z). Runs 11, 12 and 14 had high f_z in common, which may have caused the growth in forces. In addition, F_p is also related to the depth of cut (a_p) and the tool-tip radius (r_ε): the larger the a_p/r_ε, the more stable the cutting will be, contributing to a lower F_p. Thus, $a_p/r_\varepsilon = 1.5$ helps maintain lower F_p values even though other factors, mainly high f_z, contribute to an overall increase in machining forces [31]. Similar values of F_a and F_p were again observed for all lubricooling conditions.

A significant increase in the force values was not observed in Fig. 2 and Fig. 3 during the end milling of Hardox® 450 steel using the control runs (3#, 8#, 13#), confirming the hypothesis of the influence of tool wear on the machining force. No significant visual tool wear was observed in the

present study, in contrast to [5], in which flank wear was present on the cutting edge, affecting the force values. Tool wear is a factor that not only affects machining forces but also reflects on the quality of the surface finish, as it impacts the cutting-edge geometry. Thus, maintaining stable average force values and the absence of significant tool wear indicates a tendency toward a steady process resulting from the correct machining parameters, ensuring surface finish quality throughout the cutting tool's lifespan [9][10].

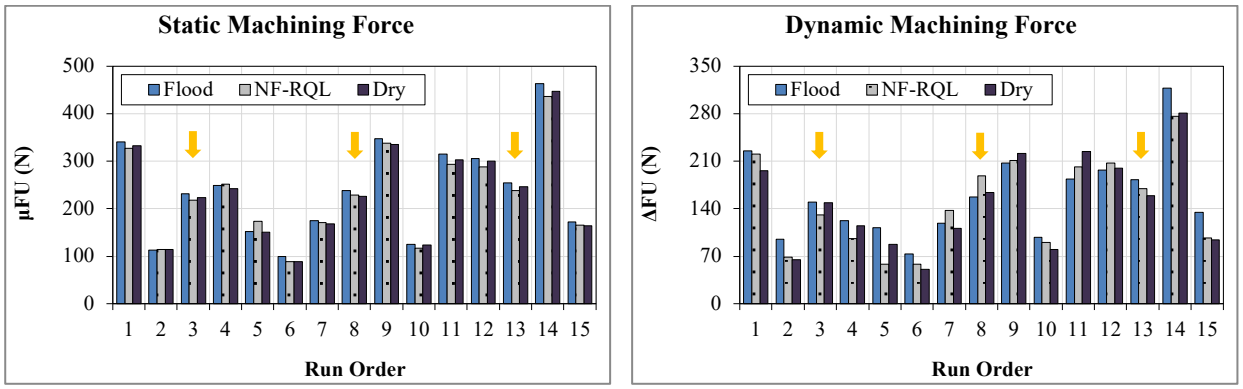

(a) (b)

Fig. 2. Machining forces for each lubricooling condition: (a) static; (b) dynamic. The orange arrows indicate the control runs 3#, 8# and 13#.

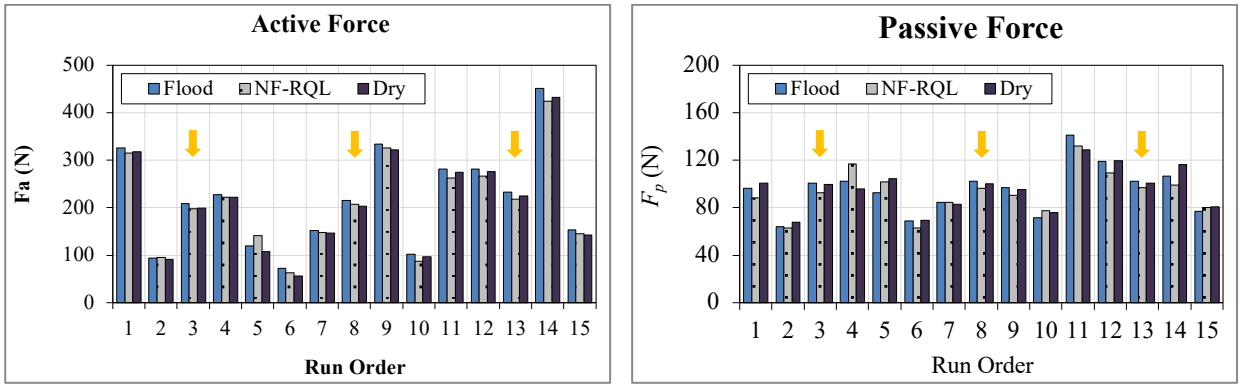

(a) (b)

Fig. 3. Machining force components for each lubricooling condition: (a) active force; (b) passive force. The orange arrows indicate the control runs 3#, 8# and 13#.

Table 3 presents the statistical variance calculated in the force values generated on the control runs (3#, 8#, 13#), aiming to understand the stability of the process, i.e., verify the influence of external factors on the results. The highest variations were observed for ΔF_U in NF-RQL and flood machining, presenting itself as the most sensitive parameter to the uncontrollable variables of the process. The lowest variations were noted for F_p in dry and flood conditions, proving to be the most stable. According to Anderson et al. [32], the machining force variations are directly linked to process vibrations, resulting in chip thickness variations that lead to new vibrations in end milling. Therefore, high variations in portions or components of machining force may indicate instabilities in the process not observed here.

Table 4 shows the reduced analysis of variance (ANOVA) performed to understand the linear, quadratic, and combined effects of the cutting parameters (controllable factors) on the analyzed forces (response variables). The reduced ANOVA presents only the controllable factors considered significant on the response variables with a p-value ≤ 0.05 (confidence interval equal to or greater than 95%) and "almost significant" (typed in gray) with 0.05 < p-value ≤ 0.10 (confidence interval between 90% and 95%). Significant factors indicate a high likelihood that the observed differences in the response variables are due to these factors rather than occurring by chance. In contrast, the almost-significant factors exhibit an influence close to being statistically significant but did not reach the usual significance level of 0.05.

Table 3. Statistical variance of the force values for runs 3#, 8# and 13#.

Response variable	Flood	NF-RQL	Dry
μF_U	9.6%	8.6%	10.6%
ΔF_U	20.7%	35.6%	9.9%
F_a	11.4%	9.5%	12.8%
F_p	2.0%	4.6%	1.1%

Table 4. Reduced ANOVA of forces for the lubricooling conditions

Input factor	μF_U						ΔF_U					
	Flood		NF-RQL		Dry		Flood		NF-RQL		Dry	
	p-value	Pr (%)	p-value	Pr (%)	p-value	Pr (%)	p-value	Pr (%)	p-value	Pr (%)	p-value	Pr (%)
a_p	< 0.001	70.2	< 0.001	71.6	< 0.001	69.9	< 0.001	55.0	< 0.001	53.4	< 0.001	54.7

f_z	< 0.001	24.8	< 0.001	25.9	< 0.001	26.0	0.002	29.5	0.002	23.9	< 0.001	34.6
a_p^2	-	-	-	-	-	-	-	-	0.067	-	0.002	2.31
$v_c \times f_z$	-	-	-	-	-	-	-	-	-	-	0.029	0.65
$v_c \times a_p$	-	-	-	-	-	-	-	-	-	-	0.029	0.64
$a_p \times f_z$	< 0.001	4.51	0.001	1.94	< 0.001	3.74	0.013	11.0	0.010	12.3	< 0.001	6.44
R^2	99.79%		99.77%		99.73%		96.19%		96.20%		99.65%	
Input factor	***F_a***						***F_p***					
	Flood		**NF-RQL**		**Dry**		**Flood**		**NF-RQL**		**Dry**	
	p-value	**Pr (%)**	**p-value**	**Pr (%)**	**p-value**	**Pr (%)**	**p-value**	**Pr (%)**	**p-value**	**Pr (%)**	**p-value**	**Pr (%)**
a_p	< 0.001	72.2	< 0.001	72.8	< 0.001	73.0	0.021	24.8	0.017	21.3	0.002	22.7
f_z	< 0.001	22.4	< 0.001	24.0	< 0.001	22.5	0.011	35.1	0.013	24.7	< 0.001	54.8
a_p^2	-	-	-	-	-	-	0.041	18.31	0.072	10.43	0.010	10.97
f_z^2	-	-	-	-	-	-	-	-	0.074	8.83	0.052	4.07
$a_p \times f_z$	< 0.001	5.01	0.001	2.77	0.001	4.07	-	-	0.026	16.82	-	-
R^2	99.74%		99.65%		99.62%		88.68%		91.34%		96.95%	

The results showed that the main factors a_p, f_z, and the interaction a_p x f_z were significant on the response variables for a confidence interval greater than 98.5% for μF_U, ΔF_U and F_a, independently of lubricooling condition applied. Depth of cut had the highest contribution, followed by feed per tooth and a_p x f_z interaction. In addition, the quadratic effect of a_p was also significant on ΔF_U in dry cutting and almost significant in the NF-RQL condition (93.3% confidence interval). This result may be related to the contribution of the depth of cut in the fluctuation of forces, this effect being more stable and less significant as the presence of cutting fluid increases. Furthermore, the interactions v_c x f_z and v_c x a_p presented significant effects only on ΔF_U in dry cutting, collaborating with the hypothesis that these combined effects contribute extensively to the fluctuation of forces with the reduction of fluid used.

The effects of the factors on F_p were quite different from the other response variables. As mentioned above, the passive force is related to process vibrations associated with the increase in the undeformed chip width and thickness as a function of the depth of cut and feed per tooth [32], in addition to several uncontrollable factors. This effect may have decreased the determination coefficient (R^2), mainly in flood and NF-RQL conditions, even at acceptable R^2 levels [33]. Despite the effects of f_z and a_p being significant and presenting higher contributions, the greatest influence was produced by feed per tooth. The quadratic effect of a_p was significant for flood and dry conditions and almost significant (92.8% confidence interval) for NF-RQL. In contrast, the quadratic effect of f_z was almost significant for NF-RQL (92.6% confidence interval) and dry (94.8% confidence interval). Finally, the a_p x f_z interaction was significant only for NF-RQL.

The results highlight the significance of factors such as a_p, f_z, and the interaction of a_p x f_z on the response variables, irrespective of the applied lubricooling conditions, with a confidence interval greater than 98.5% for μF_U, ΔF_U and F_a. Depth of cut had the most substantial impact, followed by feed per tooth and the a_p x f_z interaction. The analysis also revealed the significance of the quadratic effect of a_p, particularly in dry cutting, and the influence of factors like v_c x f_z and v_c x a_p on ΔF_U in dry cutting.

Fig. 4 shows the contour plots of the static and dynamic portions of the machining force (μF_U and ΔF_U), and Fig. 5 of the active and passive components (F_a and F_p), aiming to understand better the behavior of response variables as a function of controllable input factors. The regions with lower values are highlighted to indicate the best parameters within the evaluated range. Since the depth of cut was the most significant factor on μF_U, ΔF_U and F_a, the a_p was fixed at its low level (0.40 mm). In contrast, in the F_p analysis, the feed per tooth was set at its low level (0.05 mm/tooth).

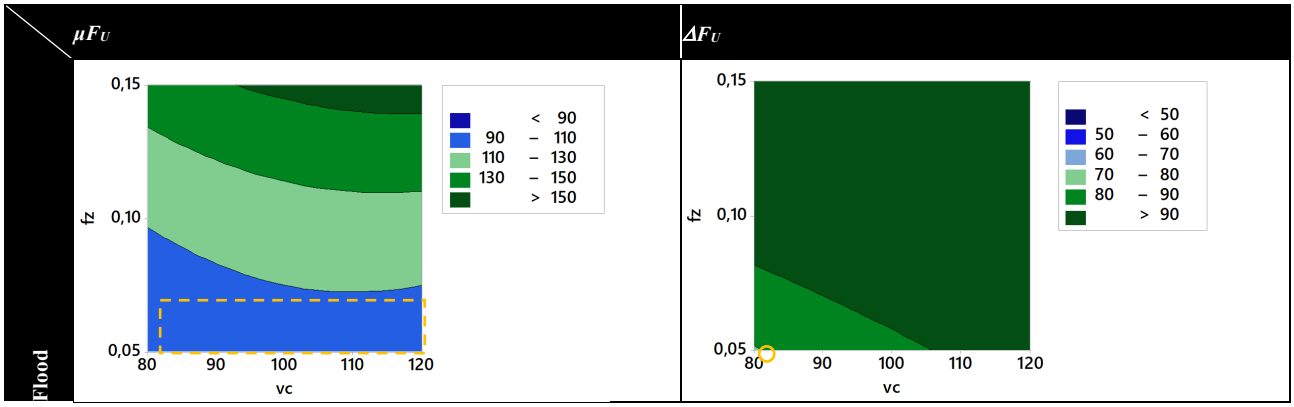

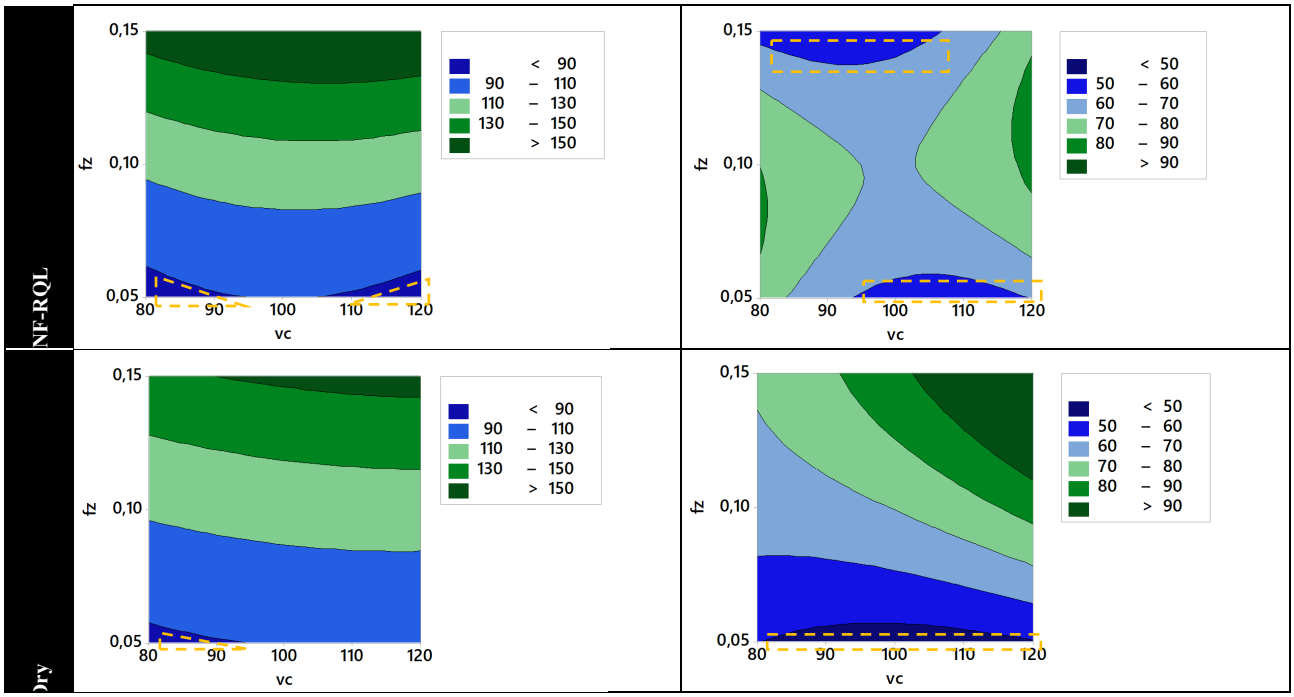

Fig. 4. Contour plots for μF_U and ΔF_U (a_p = 0.4 mm).

The significant influence of f_z on the response variables for the different levels of v_c was observed in Fig. 4. The comparison between the lubricooling environments for μF_U shows little expressive differences in the pattern of the variations of the contour bands. However, unlike the others, the lowest μF_U values in the flood condition were between 90 N and 110 N for f_z = 0.07 mm/tooth at any level of v_c. In this technique, it is observed that the speed does not affect the force values for the range of evaluated parameters, possibly due to the lubricating effects. However, the cooling effects may have resulted in a higher mean value of the forces in the optimal region than the other methods. This factor may be linked to the work hardening of the material at relatively low temperatures [34]. The lowest μF_U values in dry cutting (below 90 N) were achieved for $v_c \leq 90$ m/min and low f_z (0.05 mm/tooth), while in NF-RQL milling, such values were obtained with low f_z and $v_c \leq 90$ m/min or $v_c \geq 110$ m/min. The similarity in behavior between NF-RQL and dry may be linked to the effects of low cooling in the cutting zone. However, the lubricating effects of NF-RQL make it possible to work in higher speed ranges. The observed performance for cutting speed in the use of nanofluid in reduced application is also reported by Duc et al. [12], which obtains a reduction in cutting forces to values above 105 m/min.

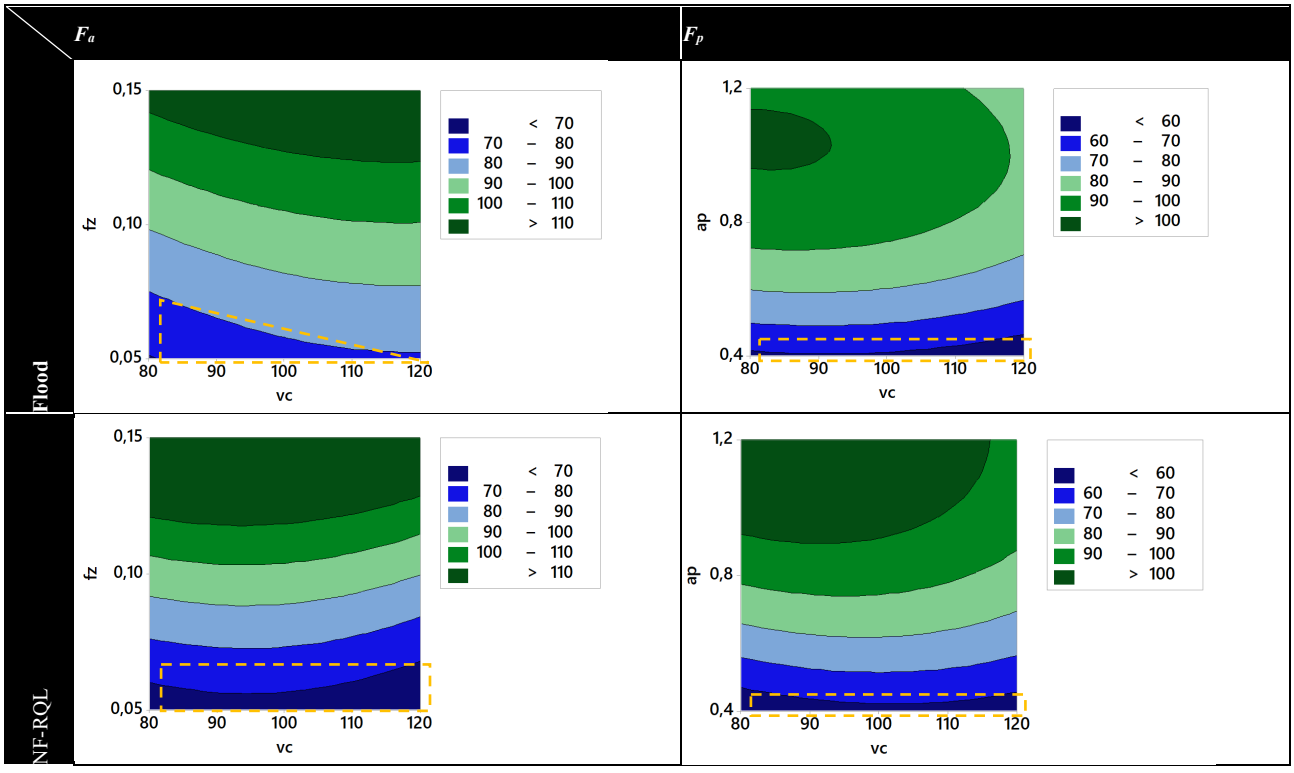

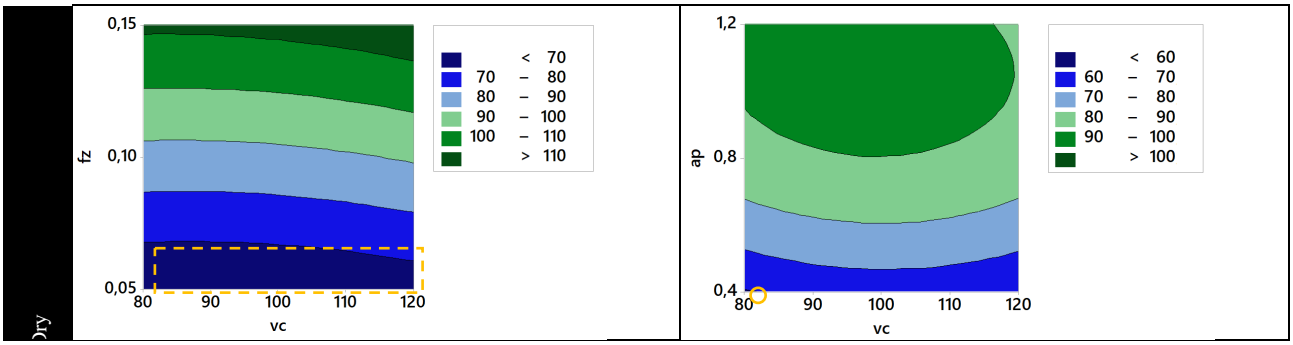

Fig. 5. Contour plots for F_a (a_p = 0.4 mm) and F_p (f_z = 0.05 mm/tooth).

For ΔF_U, differences in variations between different lubricooling strategies were evident. In flood machining, the lowest values obtained were between 70 N and 80 N, exclusively with low levels of f_z and v_c. Lower values were reached (from 50 N to 60 N) by applying NF-RQL in two situations: high f_z (0.15 mm/tooth) with $v_c \leq 105$ m/min and low f_z (0.05 mm/tooth) using $v_c \geq 95$ m/min. In this case, the smallest ΔF_U values were generated in dry cutting with low f_z for any cutting speeds in the range considered in this study. The material softening at high temperatures may have influenced the optimal region for ΔF_U. Thus, it becomes necessary to achieve an outstanding combination of cutting speed and feed per tooth so that there is less force fluctuation due to the difficulty in machining Hardox® 450 at low temperatures [34].

Considering the results obtained in each contour plot, the flood condition did not generate $\mu F_U < 90$ N, corroborating the hypothesis that low temperatures in the cutting zone do not favor the material softening conditions, helping reduce the forces. In flood, the ΔF_U values were the highest among the other lubricooling conditions, indicating a higher fluctuation, again due to the increase in work hardening with the greater cooling capacity [1]. Dry cutting and NF-RQL exhibit regions in these graphs with lower forces, whereas NF-RQL shows areas with lower μF_U even at high speeds, which may be a result of the lubricating effect caused by the effective application of the oil droplets in the cutting zone [17]. However, for ΔF_U, the work-hardening effect can have overridden the lubrication effect, resulting in a better result for dry cutting in which temperatures at the tool-chip interface are higher and, thus, less chip thickness variation and lower force fluctuation.

Analyzing the active component of the machining force (F_a), the flood condition again showed the highest force values among the approached lubricooling techniques. In this case, the smallest values (from 70 N to 80 N) were generated using the low f_z level for any v_c in the evaluated range (from 80 m/min to 120 m/min). It is also noted that higher feeds per tooth can be used (up to 0.07 mm/tooth), provided the cutting speed decreases proportionally with increasing f_z. In dry and NF-RQL conditions, smaller F_a values (below 70 N) were produced for low levels of feed per tooth ($f_z < 0.6$ mm/tooth) at any v_c. Except for dry milling that requires low v_c (80 m/min), the smallest F_p values (less than 60 N) were obtained in flood and NF-RQL machining using lower a_p (0.4 mm) across the assumed v_c range. The effect of the cross-sectional area on the F_a results was again noted because, in all lubricooling conditions, the variation of f_z becomes more significant than the change in cutting speed. A similar effect was observed in the passive component (F_p); however, the dry condition presented a tiny region in the graph (v_c = 80 m/min), indicating lower forces. A lower tribological state than the other lubricooling conditions possibly contributes to the increase in the F_p [31].

The contour plots shown in Fig. 4 and Fig. 5 aim to understand better the behavior of response variables concerning controllable input factors. They highlight regions with lower values, indicating the most favorable parameters within the assessed range. The choice of fixed parameters, such as a_p and f_z, depended on their significance and impact on specific force components (μF_U, ΔF_U, F_a, and F_p). These analyses help comprehend the relationship between controllable factors and response variables, shedding light on the best machining conditions for Hardox® 450 steel. The influence of f_z on response variables across different cutting speeds (v_c) was evident in Fig. 4. The results reveal variations in force patterns based on different lubricooling strategies and cutting conditions, affecting μF_U and ΔF_U differently. It's observed that lubricating and cooling effects have distinct impacts on force values, influencing the optimal regions for machining.

Aiming to obtain the lowest machining forces for all response variables simultaneously, Tab. 5 presents the results of the multivariate optimization performed via Minitab® 18 for each lubricooling condition. As expected, the values resulting from the optimization show slight differences in the controllable input factors, establishing the minimum levels of f_z and a_p for all lubricooling conditions. However, v_c varied among these conditions (low level for flood, about 10% higher than the low level for dry, and approximately 5% lower than the high level for NF-RQL). This higher cutting speed estimated by the model for NF-RQL is justified. Although v_c did not significantly affect the force values according to ANOVA, the contour plot of NF-RQL showed regions of lower forces for higher levels of v_c. According to Chinchanikar et al. [29], adding nanoparticles can explain this effect by improving tribological states. Thus, when comparing the optimized cutting parameters, the material removal rate with NF-RQL (1456 cm^3/min) is higher than dry (1116 cm^3/min) and flood (1019 cm^3/min) conditions, improving productivity.

The discovery that using nanofluids in NF-RQL conditions can enhance material removal rates, boosting productivity and resulting in lower machining forces, is promising in terms of energy and environmental efficiency. Furthermore, it represents a significant reduction in environmental impact compared to the flood cutting (flow rate of 540 l/h to 2.0 l/h), offering an eco-friendly approach to machining the Hardox®.

Regarding economic aspects, other factors, such as the cost and consumption of NF-MLG in RQL compared to BD-Fluid B90 in abundance, need to be evaluated. There are challenges to be overcome in nanofluids [21] or even cutting tool costs applied in dry machining in which the tool coating can significantly influence the process performance [15]. There is also a slight variation in the predicted results,

oscillating between the smallest and largest values of each portion of the machining force for each lubricooling condition. Run 6 (v_c = 100 m/min, f_z = 0.05 mm/tooth, a_p = 0.40 mm) used low feed levels per tooth and depth of cut the same as the optimized values, differing only in the cutting speed (non-significant parameter). The experimental values obtained in this run were similar to those predicted through optimization, with the practical ones slightly higher.

4. Conclusions

This work investigates the effect of the cutting parameters and NF-RQL application of a multilayer graphene-based nanofluid on the machining forces generated during the end milling of Hardox® 450 when compared to flood and dry conditions. From the results obtained, the main conclusions are pointed out below.

- There are low differences in the force values among the lubricooling conditions applied (flood, NF-RQL, and dry). However, forces depend mainly on the cutting parameters and their interactions with the lubricooling environment.
- ANOVA showed that the static (μF_U) and dynamic (ΔF_U) machining force portions and the active machining force component (F_a) have the same behavior for all lubricooling conditions. The depth of cut (a_p) is the most significant parameter, followed by feed per tooth (f_z) and the interaction between them. The passive component (F_p) presented a different behavior that varied with the lubricooling strategy.
- Contour plots showed regions with smaller values of μF_U, ΔF_U, F_a, and F_p for the lower levels of a_p and f_z, considering the suitable cutting speed (v_c) according to the lubricooling technique. This variation of v_c was proven in the multivariate optimization, in which the NF-RQL generated the highest value (114.34 m/min) and the flood condition the lowest (80 m/min).
- Experimental results and those estimated by the model did not highlight an optimal lubricooling condition for all the analyzed response variables. Despite this, a higher v_c in NF-RQL milling improves productivity due to a higher material removal rate and supports the ecological aspects inherent to this method, significantly reducing the amount of fluid used compared to the flood condition.
- Based on the results, a practical recommendation for the machining industry is to use cutting parameters within the recommended ranges, reducing the cutting forces and energy consumption. Implementing the NF-RQL technique for environmental impact reduction and increased productivity is also advised, as the optimal parameters' levels are higher than the others.
- A more in-depth analysis of the economic aspects of implementing the technique is recommended for future work. A detailed environmental impact assessment can also be conducted, possibly replicating the tests using vegetable-based cutting fluids, which may further enhance the eco-friendly approach.

Acknowledgments

The authors thank TMSA Co. for the Hardox® 450 steel, Walter Tools for the cutting tools, Bondmann Chemistry for the BD-Fluid B90, Micromazza Co. for the chemical composition analysis, Laboratory of Thin Films and Plasma Processes (LFFPP) at Federal University of Triângulo Mineiro (UFTM) for the graphene-based nanofluid, and Capes (Grant no. 88887.495511/2020-00) for student scholarship.

References

[1] K. Bensaid, H. Dhiflaoui, H. Bouzaiene, H. Yahyaoui, and N. B. Fredj, "Effects of the cooling mode on the integrity and the multi-pass micro-scratching wear resistance of Hardox 500 ground surfaces," *Int. J. Adv. Manufact. Techn.*, vol. 113, no. 9, pp. 2865–2882, Apr. 2021, doi: 10.1007/s00170-021-06719-x.

[2] SSAB., *Welding Handbook: A Guide to Better Welding of Hardox and Strenx*, 2. ed. SSAB, Oxelösund, 2019.

[3] C. Löwgren, V. Orpana, G. Löwgren, "Three successive models for selection of materials. case: wear resistant steels". *19th Int. Conf. Produc. Res.*, SSAB Oxelösund, Sweden, 2000.

[4] "SSAB Hardox® 450 Data Sheet, 2 f. 2014." Accessed on 17 Feb. 2020. Available: http:/www.ssab.com.br/products/brands/hardox/products/hardox-450/.

[5] É. S. Passari, H. J. Amorim, and A. J. Souza, "Multi-objective optimization of cutting parameters for finishing end milling Hardox® 450," *ITEGAM-JETIA*, vol. 8, no. 34, Art. no. 34, Apr. 2022, doi: 10.5935/jetia.v8i34.805.

[6] É. S. Passari, A. J. de Souza, and A. M. Vilanova, "Surface roughness analysis in finishing end milling of Hardox® 450 steel using multilayer graphene-based nanofluid," *J Braz. Soc. Mech. Sci. Eng.*, vol. 45, no. 3, pp. 147, Feb. 2023, doi: 10.1007/s40430-023-04069-1.

[7] K. Bensaid and N. B. Fredj, "Influence of Sliding Speed and Normal Loads on the Wear Resistance of Hardox 500 Steel Ground Surfaces," in *Adv. Mech. Eng., Mat. Mech.*, M. Kharrat, M. Baccar, and F. Dammak, Eds., in Lecture Notes in Mechanical Engineering. Cham: Springer International Publishing, 2021, pp. 84–90. doi: 10.1007/978-3-030-52071-7_12.

[8] SSAB, *Machining recommendations for Hardox®,* SSAB, Oxelösund, 1, 2021, 32p.

[9] F. Klocke, *Manufacturing Processes 1: Cutting*. in RWTHedition. Berlin, Heidelberg: Springer, 2011. doi: 10.1007/978-3-642-11979-8.

[10] G. S. Upadhyaya, "Trent E.M., Wright P.K.: Metal cutting (4th edition), 'Butterworth-Heinemann', Boston, 2000," *Sci. Sinter.*, vol. 36, no. 1, pp. 54–54, 2004, Accessed: Nov. 11, 2023. [Online]. Available: https://doiserbia.nb.rs/Article.aspx?ID=0350-820X0401054U

[11] F. Kara, "Optimization of cutting parameters in finishing milling of Hardox 400 steel", *Int. J. Anal., Experim. Fin. Elem. Analys.*, vol. 5 no. 3, pp. 44-49, 2018.

[12] T. M. Duc, T. T. Long, and T. Q. Chien, "Study of cutting forces in hard milling of hardox 500 steel under MQCL condition using nano additives," *Int. J. Mech. Eng.*, vol. 6, Nov. 2019, doi: 10.14445/23488360/IJME-V6I11P101.

[13] J. Majerík and I. Barényi, "Experimental investigation into tool wear of cemented carbide cutting inserts when machining wear resistant steel Hardox 500," *Engin. Rev.*, Apr. 2016, Accessed: Nov. 11, 2023. [Online]. Available: https://www.semanticscholar.org/paper/Experimental-investigation-into-tool-wear-of-when-Majer%C3%ADk-Bar%C3%A9nyi/151559a123286ccdcf6ae25e7439da13ae6ea4a3

[14] V. P. Astakhov, "Ecological Machining: Near-dry Machining," in *Machining: Fundamentals and Recent Advances*, J. P. Davim, Ed., London: Springer, 2008, pp. 195–223. doi: 10.1007/978-1-84800-213-5_7.

[15] S. Debnath, M. M. Reddy, and Q. S. Yi, "Environmental friendly cutting fluids and cooling techniques in machining: a review," *J.*

Clean. Product., vol. 83, pp. 33–47, Nov. 2014, doi: 10.1016/j.jclepro.2014.07.071.

[16] A. Shokrani, V. Dhokia, and S. T. Newman, "Environmentally conscious machining of difficult-to-machine materials with regard to cutting fluids," *Int. J. Mach. Tools Manufact.,* vol. 57, pp. 83–101, Jun. 2012, doi: 10.1016/j.ijmachtools.2012.02.002.

[17] U. S. Dixit, D. K. Sarma, and J. P. Davim, *Environmentally Friendly Machining*. in Springer Briefs in Applied Sciences and Technology. Boston, MA: Springer US, 2012. doi: 10.1007/978-1-4614-2308-9.

[18] G. S. Goindi and P. Sarkar, "Dry machining: A step towards sustainable machining – Challenges and future directions", *J. Clean. Product.*, vol. 165, pp. 1557–1571, nov. 2017, doi: 10.1016/j.jclepro.2017.07.235.

[19] H. Tschätsch, *Applied Machining Technology*. Berlin, Heidelberg: Springer, 2009. doi: 10.1007/978-3-642-01007-1.

[20] J. Sun, Z. Huang, J. Zhao, and K. Yan, "Nano-laminated graphene-carbide for green machining," *J. Clean. Product.*, vol. 293, pp. 126158, Apr. 2021, doi: 10.1016/j.jclepro.2021.126158.

[21] S. Chinchanikar and S. K. Choudhury, "Machining of hardened steel—Experimental investigations, performance modeling and cooling techniques: A review," *Int. J. Mach. Tools Manufact*, vol. 89, pp. 95–109, Feb. 2015, doi: 10.1016/j.ijmachtools.2014.11.002.

[22] S. Chinchanikar, S. S. Kore, e P. Hujare, "A review on nanofluids in minimum quantity lubrication machining", *J. Manufact. Proc.*, vol. 68, pp. 56–70, ago. 2021, doi: 10.1016/j.jmapro.2021.05.028.

[23] R. F. Garcia, E. C. Feix, H. T. Mendel, A. R. Gonzalez, and A. J. Souza, "Optimization of cutting parameters for finish turning of 6082-T6 aluminum alloy under dry and RQL conditions," *J Braz. Soc. Mech. Sci. Eng.*, vol. 41, no. 8, pp. 317, Jul. 2019, doi: 10.1007/s40430-019-1826-4.

[24] S. L. C. Ferreira *et al.*, "Box-Behnken design: An alternative for the optimization of analytical methods", *Anal. Chim. Acta*, vol. 597, no 2, pp. 179–186, ago. 2007, doi: 10.1016/j.aca.2007.07.011.

[25] M. R. Policena, C. Devitte, G. Fronza, R. F. Garcia, and A. J. Souza, "Surface roughness analysis in finishing end-milling of duplex stainless steel UNS S32205," *Int J Adv Manuf Technol*, vol. 98, no. 5, pp. 1617–1625, Sep. 2018, doi: 10.1007/s00170-018-2356-4.

[26] D. De Oliveira, R. B. Da Silva, and R. V. Gelamo, "Influence of multilayer graphene platelet concentration dispersed in semi-synthetic oil on the grinding performance of Inconel 718 alloy under various machining conditions," *Wear*, vol. 426–427, pp. 1371–1383, Apr. 2019, doi: 10.1016/j.wear.2019.01.114.

[27] D. C. Montgomery, *Design and Analysis of Experiments*. John Wiley & Sons, 2017.

[28] J. T. Black, "Introduction to machining processes". In: *Metals Handbook: Machining*, 9. ed., ASM International, New York. 1995.

[29] D. Cica, H. Caliskan, P. Panjan, and D. Kramar, "Multi-objective Optimization of Hard Milling Using Taguchi Based Grey Relational Analysis," *Tehnički vjesnik*, vol. 27, no. 2, pp. 513–519, Apr. 2020, doi: 10.17559/TV-20181013122208.

[30] J. P. Davim, Ed., *Machining of Hard Materials*. London: Springer, 2011. doi: 10.1007/978-1-84996-450-0.

[31] C. E. H. Ventura, H. S. Chaves, J. C. Campos Rubio, A. M. Abrão, B. Denkena, and B. Breidenstein, "The influence of the cutting tool microgeometry on the machinability of hardened AISI 4140 steel," *Int J Adv Manuf Technol*, vol. 90, no. 9, pp. 2557–2565, Jun. 2017, doi: 10.1007/s00170-016-9582-4.

[32] C. S. Anderson, S. E. Semercigil, e Ö. F. Turan, "A passive adaptor to enhance chatter stability for end mills", *Int. J. Mach. Tools Manufact*, vol. 47, nº 11, pp. 1777–1785, set. 2007, doi: 10.1016/j.ijmachtools.2006.06.020.

[33] D. S. Moore, W. I. Notz, M. A. Flinger, *The Basic Practice of Statistics*. 7. ed., W.H. Freeman, New York, 2015.

[34] S. Chinchanikar and S. K. Choudhury, "Machining of hardened steel—Experimental investigations, performance modeling and cooling techniques: A review," *Int. J. Mach. Tools Manufact.* vol. 89, pp. 95–109, Feb. 2015, doi: 10.1016/j.ijmachtools.2014.11.002.